Enhanced physical and optoelectronic properties of Ag-doped SnS thin films

A. G. Kumar [a,*], V. K. V. Krishna [b], A. P. Lingaswamy [c], S. Masma [d], G. Prathibha [e], G. Sujatha [f], P. S. Kumar [g], T. V. Kumar [h], J. V. V. N. K. Rao [i], B. H. Rao [a]

[a] *Dept. of H&S (Physics), Gokaraju Rangaraju Institute of Engineering & Technology(A), Hyderabad-500090, T.S., India*
[b] *Dept. of Physics, Malla Reddy Engineering College(A), Hyderabad-500100, T.S., India*
[c] *Department of Physics, G. Pulla Reddy Engineering College(A), Kurnool-518007, A.P., India*
[d] *Dept. of H & S (Chemistry), St. Peter's Engineering College(A), Hyderabad-500100, T.S., India*
[e] *Dept. of Physics, CMR College of Engineering & Technology(A), Kandlakoya, Hyderabad-501401, T.S., India*
[f] *Dept. of Freshman Engineering, Audisankara college of engineering, Gudur-524101, A.P., India*
[g] *Dept. of H & S (Physics), St. Peter's Engineering College(A), Hyderabad-500100, T.S., India*
[h] *Department of Physics, CVR College of Engineering(A), Hyderabad-501510, T.S., India*
[i] *Dept. Of Physics, P.S. Govt. Degree College, Penukonda-515110, Sri Satya Sai Dist., A.P., India*

SnS thin films doped with two atomic % Ag are deposited on a pyrex glass substrates using chemical bath deposition method. The impact of 2 atomic % silver doping on the physical properties of SnS thin films is studied. X-ray diffraction studies confirmed that the deposited SnS films were of α-SnS phase with an orthorhombic crystal structure, which remained stable despite the addition of 2 at.% silver. It is observed that the addition of 2 atomic % silver to SnS chemical bath solution does not greatly influence the structural properties of SnS thin film. The deposition is carried out at different bath temperatures from 50°C to 80°C. Additionally, structural parameters such as crystallite size, dislocation density, and lattice strain were analyzed, offering deeper insights into the quality and structural properties of the SnS films.

(Received November 27, 2024; Accepted February 6, 2025)

Keywords: Ag-Doped SnS, Chemical bath deposition, Structural properties, optical properties.

1. Introduction

The energy resources of India are under immense pressure due to the country's significant and persistent economic growth. This expansion of the energy sector should properly be guided by a long term and comprehensive policy. Such a policy is framed in the Integrated Energy Policy Report of 2024. In recent years, India's natural gas besides crude oil production rate has not witnessed considerable growth. This scenario is leading to a widening gap between the energy demand and the actual supply. The obvious way out is to depend on imports. Increasing the contribution of renewable sources of energy to the country's energy sector is a perfect solution to reduce the dependency on imports. Both the Government of India and the respective state

* Corresponding author: sampath85ags@gmail.com
https://doi.org/10.15251/CL.2025.222.143

governments adopted a strategy to encourage the renewable sources of energy in the form of nuclear energy, wind mills, solar energy etc. in general. In particular, the country's solar power potential is estimated to be about 748990 MW which is about 35.5% of the estimated potential of renewable power in India.

The Energy statistics India 2024 report says that the estimated potential of renewable power in India as on 31 March 2023 is about 2109655 MW (Fig 1). The states of Andhra Pradesh and Telangana have 38440 MW and 20410 MW of Solar energy potential respectively [1]. The fact that as much as $7.45X10^{17}$ kWh of solar energy falls on the earth annually, drives the scientific community to exploit this affluent and eternal source. Conversion of solar energy into electrical energy is taken care of by Photovoltaic technology. This technology has numerous technical and social advantages. The photovoltaic systems have the following distinctive characteristics that make these systems preferable over others [2]. The photovoltaic systems:

I. Are quiet
II. Need little or no maintenance
III. Can physically be located closer to the load
IV. Are ecofriendly in operation.

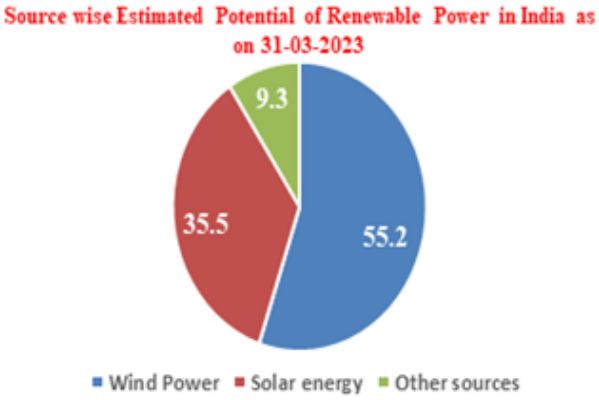

Fig. 1. Estimated potential of renewable power in India as on 31-03-2023[1].

In this context solar photovoltaics have a vital role to play. There is a good interest shown on photovoltaics from the past few decades [3]. Solar photovoltaics now forms a reliable alternative energy source in replacing not only the oil but also the coal. Concern towards ecology and pollution also is another main reason for the keen interest shown on "Solar Photovoltaics". 'Photo' in Greek means light and Photovoltaics hence means emf or voltage due to light. In other words, the process of converting solar energy into electrical energy is known as photovoltaic effect.

A Solar cell or in another words photovoltaic cell is essentially a p - n junction device. The following processes are involved in a solar cell:

i. Photons are absorbed by the material that forms the junction, due to which charge carriers are generated (Charge generation).
ii. The generated charge carriers are then separated at the junction (Charge separation).
iii. Then, these charge carriers get accumulated at the terminals (Charge collection).

Thin film hetero junction solar cell consists of a substrate that holds different layers like TCO, buffer, absorber, windows layer etc.,[4]. A very vital member in the Solar cell structure is the Absorber layer in which light absorption and carrier generation take place. In order that maximum Solar radiation is absorbed, besides minimizing the reverse saturation current density, it is necessary that the band gap of the absorber layer should be about 1.5 eV. High absorption coefficient coupled with direct band gap and p – type conductivity will be a great advantage for the absorber layer. The prominent absorber materials are GaAs, InP, CdTe, $CuInGaSe_2$ and SnS.

Among them SnS has got an edge over the other materials as the precursors of this are abundantly available and SnS is environment friendly. SnS is one among the binary compounds that belong to IV - VI group. Much like Germanium Selenide (GeSe), Germanium Sulfide (GeS), and Tin Selenide (SnSe), tin sulfide is also exhibiting layered structure, with weak Van der Waal's forces involved in coupling the different layers. Owing to these weak forces, SnS provides intrinsically a chemically inert surface without surface density states and dangling bonds [5,6]. Obviously, SnS is inert both environmentally and chemically. SnS exhibits strong anisotropic vibrational properties due to the layered structure [7,8].

2. Experimental

In the present work, the reagents as used by Pramanik et al. [9] was used and AgCl was used as dopant source. $SnCl_2.2H_2O$ is preferred to $SnCl_4.5H_2O$ for the reason that the former consists of 52.9% Sn while the latter consists of only 33.9% Sn. The chemical bath solution was prepared using 0.1M $SnCl_2.2H_2O$, 15 ml of Triethanolamine (TEA), 8 ml of Ammonia and 0.1M of Thioacetamide. 15 ml Glacial acetic acid was heated to 373K and 1.13 gm of $SnCl_2.2H_2O$ was added to it. Continuing the heating process the solution was thoroughly mixed with the clean glass stirrer. A clear and homogeneous solution was obtained. Heating was continued for about 180 seconds. 10 ml of deionized water was added to the solution and the heating and stirring continued for another 120 seconds. Then the beaker was placed on a magnetic stirrer and 25 ml of deionized water was added to the solution to make it up to 50 ml and to obtain 0.1M $SnCl_2.2H_2O$. Uniform stirring was done for another 180 seconds with the help of magnetic bead, till the entire solution is properly mixed and a clear and homogeneous solution is obtained. Then this solution was kept aside for cooling. 0.375 gm of Thioacetamide was added to 50 ml deionized water collected in a beaker. The solution was thoroughly stirred with the help of magnetic bead and magnetic stirrer for about 240 seconds till the entire thioacetamide dissolved in water and a perfectly clear 0.1 M solution was obtained. 5 ml of 0.1M $SnCl_2.2H_2O$ was collected in a 100 ml well cleaned and dried beaker. 15 ml of TEA was added and the mixture is vigorously stirred till the homogeneous solution is obtained. 8 ml of Ammonia was added to this solution and stirring was continued. After a clear and homogeneous solution was obtained, 5 ml of 0.1M thioacetamide was added to this mixture. The amount of silver chloride (AgCl) calculated from the ratio, y = [Ag] / [Sn] = 2% was added to the bath solution to account for silver doping. As the stirring continued, the initially clear and water like solution slowly changed into dark brown. Temperature setting was done to obtain the required temperature for the bath solution. The temperature was monitored using a thermometer. Once the required temperature was reached, a thoroughly cleaned, degreased glass slide was inserted into the solution such that the slide made roughly 45 – 50o angle with the walls of the beaker. This way of inclined arrangement of slide supported proper deposition of thin film on the glass substrate and was suggested by Rani et al. [10]. Depositions were carried out at four different bath temperatures i.e., T_b = 50°C, 60°C, 70°C and 80°C. The substrates were set for aerial drying for 24 hours after deposition and then annealed in a muffle furnace at 250°C for half an hour. The substrates were taken out of the muffle furnace after the temperature inside the muffle furnace got reduced to the room temperature.

3. Results and discussion

The as-prepared 2 at. % Ag-doped SnS layers were examined using XRD to know the structural properties. Structural parameters like crystallite size, dislocation density, phase identification and strain were determined from the XRD data. The as-grown Ag doped SnS layers grown at bath temperatures T_b = 50°C, 60°C, 70°C and 80°C appeared uniform, blackish brown in color, and pin - hole free. These films were well adherent to the substrate surface and no cracks were visible. The X - ray diffraction spectra was recorded for the as-grown Ag-doped SnS layers using Advanced X - ray diffractometer named Bruker D8, in the 2θ range, 20°–80°, in steps of 0.02°. The XRD patterns of as - grown layers at different bath temperatures are illustrated in the

figure 2. The XRD analysis indicated the presence of peaks at 23.1° that correspond to (110) planes. Further, the layers grown at bath temperatures 50°C, 60°C and 70°C showed a shoulder peak that corresponded to (040) plane. This peak eventually got suppressed in the case of 80oC bath temperature. These peaks coincided with the peaks in the JCPDS card file (Card number 32 - 1361), which indicates the existence of α - SnS phase with orthorhombic crystal structure. No other peaks related to SnS structure were found in the X-ray diffraction spectra. Secondly, Ag-related secondary phases were not observed in the above spectra. One interesting observation from the XRD spectra was that the incorporation of silver did not change the crystal structure of SnS. As the silver was added in low concentration, they would have either been absorbed by the grain boundaries or would have been accommodated in interstitial sites [11].

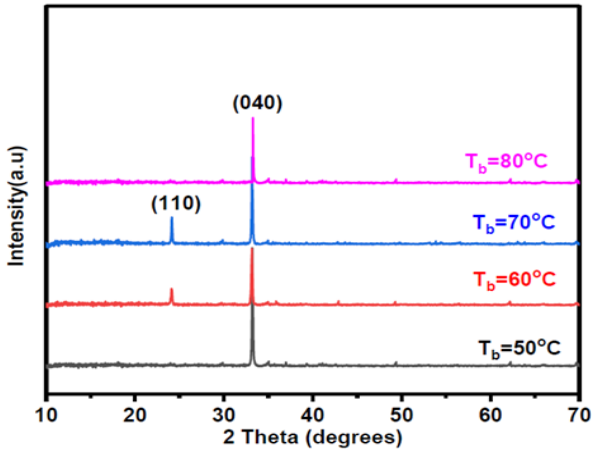

Fig. 2. XRD patterns of Ag-doped SnS layers deposited at different T_b (50°C, 60°C 70 °C and 80°C, respectively).

The evaluated lattice parameters were a = 4.185 Å, b = 11.42 Å and c = 4.13 Å. The interplanar spacing, d = 3.92 Å. The intensity of (110) peak increased with the increase in bath temperature from 50°C to 70°C. Above this temperature, at T_b = 80°C, the intensity of (110) peak decreased. T.S. Sajeesh et al. [12] reported the similar changes in the crystallinity, for the SnS layers grown using chemical bath beposition process, at different bath temperatures. Kumar et al. [13] could get the similar results for the SnS layers grown by electrodeposition process. Silver doped SnS layers were grown by pulsed electro deposition method by Y. Yongli et al. [14] and they too reported similar results. The position of (110) was unaltered, with the increase in the bath temperature, this indicated that the structure of as - grown Ag -doped SnS layers remained same, in spite of the change in bath temperature in the range 50°C – 80°C. No other secondary phases of tin sulphide like SnS_2 and Sn_2S_3 were observed in the spectra. Debye - Scherrer formula [15,16] was used to evaluate the average crystallite size (D) of the Ag-doped SnS layers. (110) was used as the preferred orientation. Also, the dislocation density (δ)[10] and the strain (ε)[17] were calculated using appropriate formulae.

Fig.3 represents the plot for crystallite size variation and dislocation density variation with respect to bath temperature in the range of 50°C – 80°C. The evaluated D value increased with the increase in bath temperature (T_b) from 50°C to 70°C and became maximum at 70°C. Coalescence of nuclei that formed the layer might be the reason for the increase of crystallite size. The increase in bath temperature results in the increase in the kinetic energy of reactants besides the accelerated interaction of various species in the bath. This increase in kinetic energy might be attributed to the increase in coalescence. At higher temperatures i.e., temperatures greater than the optimum temperature, 70°C, the interaction between the substrate surface and deposited layers got reduced due to etching process.

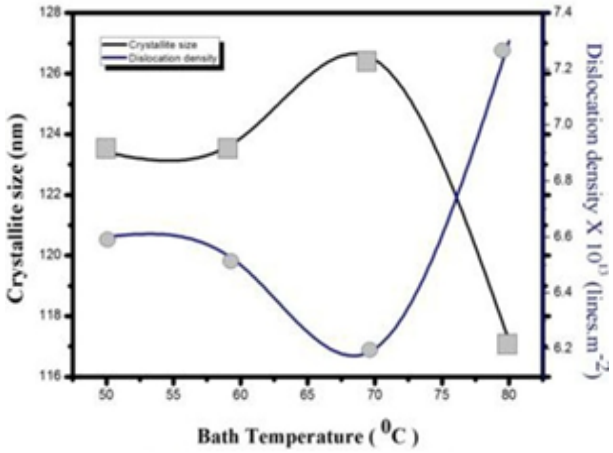

Fig. 3. Variation of Crystallite size and dislocation density with bath temperature of Ag-doped SnS thin films

The calculated dislocation density (δ) was higher at the bath temperature of 50ºC which may be due to the presence of voids besides the effect of smaller crystallite size. With the further increase in bath temperature, (δ) kept on decreasing and at the bath temperature of 70ºC, it was minimum where the crystallite size and hence crystallinity was observed to be maximum. The decrement in (δ) with the bath temperature (T_b) indicated the formation of superior-quality films at higher T_b [19]. This may be due to the reason that the dislocations received additional thermal energy and therefore got higher mobilities with the increase of T_b. These activated dislocations might have moved from the region inside the crystallites to the region in their grain boundaries and got neutralized [20,21].

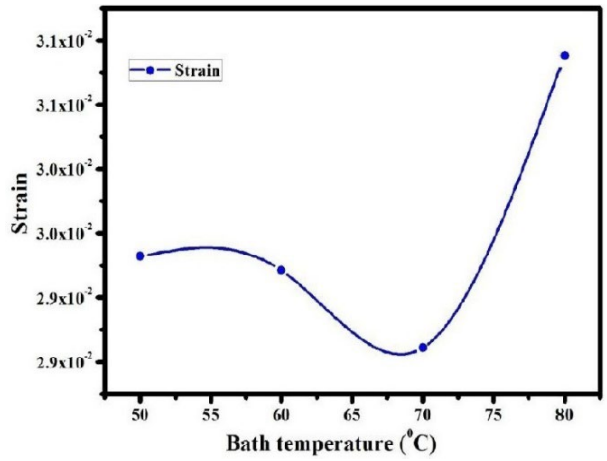

Fig. 4. Variation of Strain with bath temperature of Ag-doped SnS thin films.

Fig.4 shows the change in Strain with the change of bath temperature. The strain (ε) in the as - deposited Ag doped SnS layers was calculated using the appropriate relation. The lattice misfit between the substrate and deposited layer resulted in higher dislocation density at lower bath temperature, which further resulted in the compressive kind of strain at lower bath temperatures. The strain decreased in accordance with the dislocation density, with the increase in the bath temperature up to 70^0C and increased thereafter [22,23].

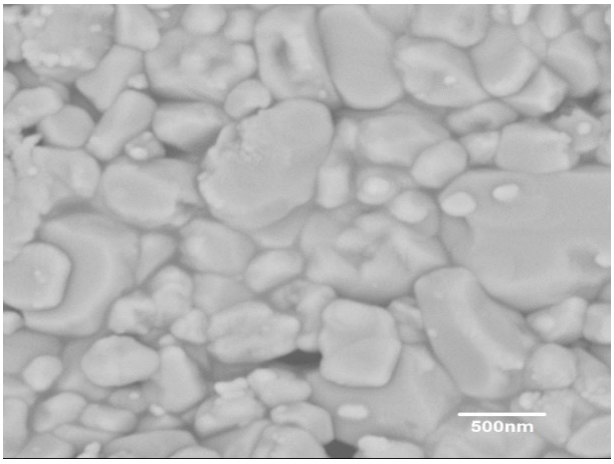

Fig. 5. Scanning electron micrograph of Ag-SnS thin films at T_b=70ºC.

Fig. 5 shows the surface morphology of Ag-doped SnS at Tb=70ºC. This SEM image reveals a granular, porous structure typical of polycrystalline materials. Captured at 16,000x magnification, the image highlights irregularly shaped particles with sizes ranging from few nm to a 500 nm. The surface of the particles is relatively smooth with minor texturing, suggesting deposition patterns characteristic of SnS. The observed morphology, with both large grains and smaller surrounding particles, suggests a broad particle size distribution [24 – 27]. This structure could be advantageous for applications such as sensors, photovoltaics, or catalysts, where high surface area is valuable.

4. Conclusions

In conclusion, X-ray diffraction studies confirmed that the deposited films were of α-SnS phase with an orthorhombic crystal structure, which remained unaffected by the addition of 2 at.% silver. The films consistently exhibited a prominent peak at 2θ = 23.1° corresponding to the (110) plane, and a secondary shoulder peak at 2θ = 31.3° related to the (040) plane, which diminished at higher bath temperatures. Notably, as bath temperature increased, the intensity of the (110) peak also increased, reaching a maximum at 70°C, indicating strong orientation along the (110) plane and optimal crystallinity at this temperature. Beyond this temperature, a decline in the (110) peak intensity was observed, suggesting decreased crystallinity. The lattice parameters were determined as a = 4.185 Å, b = 11.42 Å, and c = 4.13 Å, with an interplanar spacing of d = 3.92 Å. Structural parameters, including crystallite size, dislocation density, and lattice strain, were also evaluated, providing further insight into the quality of the SnS films.

Acknowledgements

The authors Dr. GuruSampath Kumar A. of Dept. of Physics, GRIET(A), Hyderabad and Mr. Kesava Vamsi Krishna V., of Dept of Physics, MREC(A), Hyderabad would like to appreciate the for their support and cooperation to complete my synthesis and characterization work smoothly.

References

[1] Twenty Point Programme (TPP)-2006 Annual Report 2022-23 Social Statistics Division National Statistical Office Ministry of Statistics & Programme Implementation Government of India.

[2] A.G.S. Kumar, L. Obulapathi, M. Maddaiah, T.S. Sarmash, D.J. Rani, J.V.V.N.K. Rao, T.S. Rao, AIP Conf Proc. **1665,** 080002 (2015); http://dx.doi.org/10.1063/1.4917906.
[3] D.J. Rani, A.G.S. Kumar, T.S. Sarmash, K.C.B. Naidu, M. Maddaiah, T.S. Rao, JOM. **68** 1647 (2016); https://doi.org/10.1007/s11837-016-1910-5.
[4] R. Ramadan, S. Dadgostar, M. Manso–Silván, R. Pérez-Casero, M. Hernandez Velez, J. Jimenez, O. Sanchez, Mater. Sci. Eng. B Solid State Mater. Adv. Technol., **276,** 115558 (2022); https://doi.org/10.1016/j.mseb.2021.115558.
[5] H. Zhu, D. Yang, Y. Ji, H. Zhang, S. Xiaofei, J. Mater. Sci., **40**, 591 (2005).
[6] V.S. Samyuktha, A.G.S. Kumar, T.S. Rao, R.P. Suvarna, Mater. Today Proc. **3**, 1768 (2016); https://doi.org/10.1016/j.matpr.2016.04.072.
[7] N. Spalatu, J. Hiie, R. Kaupmees, O. Volobujeva, J. Krustok, I.O. Acik, M. Krunks, ACS Appl Mater Interfaces. **11**, 17539 (2019); https://doi.org/10.1021/acsami.9b03213
[8] K.C.B. Naidu, T.S. Sarmash, M. Maddaiah, A.G.S. Kumar, D.J. Rani, V.S. Samyuktha, L. Obulapathi, T.S. Rao, J. Ovonic Res., **11**, 79 (2015).
[9] P. Pramanik, P.K. Basu, S. Biswas, Thin Solid Films, **150**, 269 (1987); https://doi.org/10.1016/0040-6090(87)90099-X
[10] D.J. Rani, A.G.S. Kumar, T.S. Rao, J. Coat. Technol. Res. **14**, 971 (2017); https://doi.org/10.1007/s11998-017-9951-4.
[11] R. Balakarthikeyan, A. Santhanam, A. Khan, A.M. El-Toni, A.A. Ansari, A. Imran, M. Shkir, S. AlFaify, Optik, **244**, 167460 (2021); https://doi.org/10.1016/j.ijleo.2021.167460.
[12] T.H. Sajeesh, K.B. Jinesh, M. Rao, C.S. Kartha, K.P. Vijayakumar, Phys. Status Solidi (A): Appl. Mater. Sci., **209**, 1274 (2012); https://doi.org/10.1002/pssa.201127442.
[13] Y. Geng, L. Wang, Y. Xu, A.G.S. Kumar, X. Tan, X. Li, Opt. Express, **26** (21), 27907 (2018); https://doi.org/10.1364/OE.26.027907.
[14] Y.L. Yang, S.Y. Cheng, S.L. Lai, Adv. Mat. Res. **60–61**, 105 (2009); https://doi.org/10.4028/www.scientific.net/amr.60-61.105.
[15] A.G.S. Kumar, L. Xuejin, Y. Du, Y. Geng, X. Hong, J. Alloys Compd., **798**, 467 (2019); https://doi.org/10.1016/j.jallcom.2019.05.227.
[16] A.G.S. Kumar, T.S. Sarmash, D.J. Rani, L. Obulapathi, G.V.V.B. Rao, T.S. Rao, K. Asokan, J. Alloys Compd., **665**, 86 (2016); https://doi.org/10.1016/j.jallcom.2016.01.029.
[17] A.G.S. Kumar, X. Li, Y. Du, Y. Geng, X. Hong, Appl Surf Sci., **509,** 144770 (2020); https://doi.org/10.1016/j.apsusc.2019.144770.
[18] R. Bayón, M. Hernández-Mayoral, J. Herrero, J. Electrochem. Soc. **149**, C59 (2002); https://doi.org/10.1149/1.1425793.
[19] S.K. Pendyala, K. Thyagarajan, A.G.S. Kumar, L. Obulapathi, J. Microw. Power Electromagn. Energy, **53**, 3 (2019); https://doi.org/10.1080/08327823.2019.1569898.
[20] D.J. Rani, A.G.S. Kumar, L. Obulapathi, T.S. Rao, IEEE Trans. Dielectr. Electr. Insul., **26**, 1134 (2019); https://doi.org/10.1109/TDEI.2019.007887.
[21] H. C. Rao Bitra, A. V. Rao, A.G.S. Kumar, G. N. Rao, Digest J. Nanomater. Biostruct., **16** (3), 1173 (2021).
[22] A.G. Kumar, X. Li, X. Hong, Y. Geng Yu Du, T.S. Rao, Radiat. Phys. Chem., **162**, 107-113 (2019); https://doi.org/10.1016/j.radphyschem.2019.02.033
[23] Y. Xu, Y. Geng, L. Wang, A.G. Kumar, L. Fang, Y. Du, X. Li, J. Phys. D: Appl. Phys. **51**, 285104 (2018); https://doi.org/10.1088/1361-6463/aacab2.
[24] A.G. Kumar, C. Mahender, U.M. Kumar, L. Obulapathi, B.H. Rao, P. Yamuna, A. Thirupathi, L.N.V.H. SomaSundar, G.V. Ramana, J. Vacc. Sci. Techol. B, **42** 052201 (2024); http://doi.org/10.1116/6.0003690.
[25] T.V. Kumar, A.S. Chary, A.M. Awasthi, S. Bhardwaj and S.N. Reddy, Ionics, **21**, 1341-1349 (2015); https://doi.org/10.1007/s11581-014-1301-2
[26] G.V.B. Rao, · U.M. Kumar, L.N.V.H. SomaSundar, K.L. Sarada, J.V. Kumar, A.G. Kumar, G.V. Ramana, B.H. Rao, L. Obulapathi, Xuejin Li,Braz. J. Phys., **54**, 120 (2024); https://doi.org/10.1007/s13538-024-01497-9.
[27] W. H. Albanda, M.H. Saeed, M.Z. Abdullah, M.H. Al-Timimi, Chalcogenide Lett., **21**, 439-447 (2024); https://doi.org/10.15251/CL.2024.215.439